Results in Physics 17 (2020) 103180

Contents lists available at ScienceDirect

Results in Physics

journal homepage: www.elsevier.com/locate/rinp

Microarticle

Processing of the Nd_2O_3:SiO_2 system by Laser Floating Zone in air

F. Rey-García[a,b,*], N.M. Ferreira[a], A.J.S. Fernandes[a], F.M. Costa[a]

[a] Departamento de Física & I3N, Universidade de Aveiro, 3810-193 Aveiro, Portugal
[b] Instituto de Ciencia de Materiales de Aragón, CSIC-Universidad de Zaragoza, María de Luna 3, E-50018 Zaragoza, Spain

ARTICLE INFO

Keywords:
Nd_2SiO_5
$Nd_{9.33}(SiO_4)_6O_2$
Laser Floating Zone
Raman spectroscopy

ABSTRACT

Highly textured polycrystalline fibres of monoclinic $P2_1/c$ Nd_2SiO_5 and hexagonal $P6_3/m$ $Nd_{9.33}(SiO_4)_6O_2$ phases were obtained by Laser Floating Zone in air from stoichiometric mixtures of Nd_2O_3 and SiO_2 changing the pulling rate from 10 to 400 mm/h. Distribution of phases barely varied due to the incongruent melt of the Nd_2O_3:SiO_2 system, resulting in fibres adequate for microwave devices owing to the dielectric character of the Nd_2SiO_5 phase. Raman analysis was performed in this material for the first time.

Introduction

Neodymium apatite-type silicates have a great technological interest since they can be employed in solid oxide fuel cells (SOFCs) or in microwave devices [1–6]. The oxygen ionic conductivity of $Nd_{9.33}(SiO_4)_6O_2$ matches and even overpasses that of yttria-stabilized zirconia (YSZ) ($\sigma = 1 \times 10^{-3}$ S/cm) [4], while the estimated dielectric constant ($\varepsilon_r = 7.94$) and Quality factor (Qxf = 38800 GHz) of Nd_2SiO_5 porous ceramics make it suitable for microwave passive components [1]. However, their production by standard methods is hard since the Nd_2O_3:SiO_2 system melts incongruently, usually causing mixtures of by-products [1–6].

Alternatively, pure $Nd_{9.33}(SiO_4)_6O_2$ single crystals were obtained from neodymium silicate pre-sintered rods by both the Floating Zone (FZ) [5] and the Laser Floating Zone (LFZ) [7] methods at low pulling rates (< 5 mm/h), under special environments (mixing argon, nitrogen and/or oxygen). Considering that Gd_2SiO_5 and Lu_2SiO_5 crystals were successfully grown by LFZ in air at 10 and 200 mm/h [8,9], respectively, this approach was also explored for the Nd_2O_3:SiO_2 system.

Experimental

Preform rods extruded from stoichiometric mixtures of Nd_2O_3 (Acros Organics, 99.9%) and SiO_2 (Aldrich, 99.6%) raw oxide powders [8,9] were irradiated with a 200 W CO_2 laser (Spectron, GSI group). Seed and feed rods were rotated in opposite directions at 5 and 15 rpm, respectively. Thus, fibres with diameters of 2 mm and 15–30 mm in length were grown by LFZ in air varying the pulling rate from 10 to 400 mm/h. Samples are denoted by the acronym *NSO* followed by the corresponding pulling rate (Table 1).

Compositional and microstructural studies were accomplished by SEM/EDX (Tescan Vega 3 SBH), XRD (EMPYREAN X-ray and Philips MRD diffractometers for powder and texture analysis, respectively) and by room temperature (RT) μ-Raman spectroscopy (Horiba Jobin-Yvon HR800) using a Kimmon IK Series He-Cd laser emitting at 441.6 nm. Finally, electrical measurements were performed using an Agilent 4292A Precision Impedance Analyser (0.1–1 MHz, 30–1000 °C in steps of 100 °C) covering the fibre's polished ends with Pt paste to provide an appropriate electrical contact.

Results

According to the XRD recorded diffractograms, crystalline violet fibres grown by LFZ were composed by monoclinic $P2_1/c$ Nd_2SiO_5 (ND2) and hexagonal $P6_3/m$ $Nd_{9.33}(SiO_4)_6O_2$ (ND9.33) phases, matching the 04-015-6879 and the 04-015-7135 ICDD (International Centre for Diffraction Data, 2020) XRD cards. On the other hand, despite the pulling rate variation, Rietveld refinement calculations show that the phase distribution barely varied (Table 1), since this system melts incongruently [1,3]. SEM/EDS analysis allowed to observe strong texturing, especially in samples pulled at > 100 mm/h, where brighter ND2 crystals appear parallelly aligned inside the darker ND9.33 matrix (Fig. 1a, b). Considering the revised phase diagram [1,3], a redistribution or a segregation process implying a possible local excess of SiO_2 occurred. Likewise, NSO-10 samples present a more disordered appearance, displaying lamellae and highly interconnected short-in-length fibrils together with a banding effect from the ND2 phase. Concomitantly, NSO-10 should be dielectric while NSO-200 and NSO-400 should be good electrical conductors due to their strong texturing [10].

* Corresponding author.
E-mail address: francisco.rey.usc@gmail.com (F. Rey-García).

https://doi.org/10.1016/j.rinp.2020.103180
Received 25 April 2020; Accepted 20 May 2020
Available online 25 May 2020

Table 1
LFZ experimental conditions and phase distribution percentages calculated from Rietveld refinement after XRD analysis.

Sample	Pulling rate	Power	Phase (%)	
	(mm/h)	(W)	ND2	ND9.33
NSO-400	400	75	34.3	65.7
NSO-200	200	73	38.9	61.1
NSO-100	100	72	40.7	59.3
NSO-10	10	69	37.2	62.8

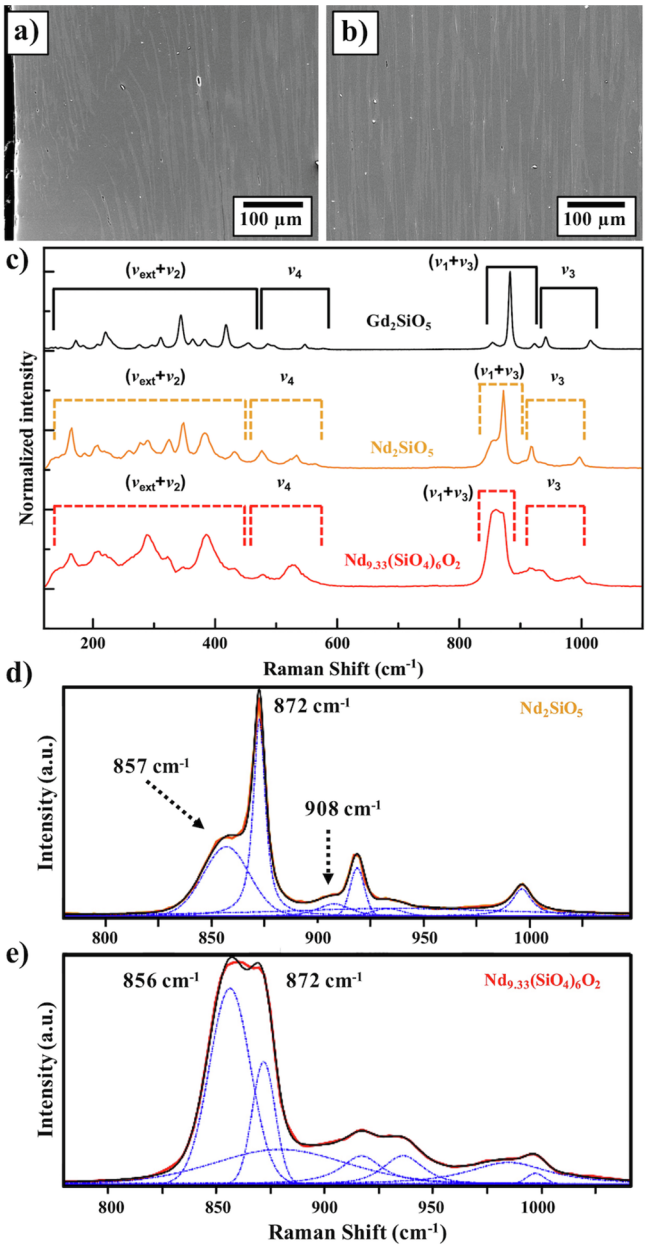

Fig. 1. SEM micrographs (500×) at outer (a) and inner (b) areas of the NSO-400 sample. c) Normalized Raman spectra of Nd_2SiO_5 (gold) and $Nd_{9.33}(SiO_4)_6O_2$ (red) phases recorded from 120 to 1100 cm^{-1} and compared to that of single-crystal Gd_2SiO_5 (black) [8]. Normalized Raman spectra of d) Nd_2SiO_5 and e) $Nd_{9.33}(SiO_4)_6O_2$ phases in the 780–1040 cm^{-1} range showing the deconvolution peaks (blue dashed), the corresponding sum (continuous black) and the experimental data (red).

Raman spectra of the Nd_2SiO_5 and $Nd_{9.33}(SiO_4)_6O_2$ phases were recorded for the first time, to our knowledge (Fig. 1c). The ND2 spectrum is comparable to that of the Gd_2SiO_5 (GSO) [8], presenting a similar number of sharp peaks in the low wavenumber region (<600 cm^{-1}), while the spectrum corresponding to the ND9.33 phase presents fewer of such features. Additionally, data fitting of the Raman spectra (Fig. 1d, e) of both phases between 780 and 1040 cm^{-1} allowed to identify the A-type typical triplet of oxyorthosilicates [8] for the ND2 phase. This is formed by a prominent sharp peak, placed at 872 cm^{-1} and is assigned to the ν_3 antisymmetric stretching vibration of the $[SiO_4]^{4-}$ tetrahedron complexes, surrounded by peaks placed at 857 and 908 cm^{-1}. Concerning to the ND9.33 phase, the Raman spectrum structure in the same region retains features from that of the ND2 phase, but with wider bands and increased background. This spectrum is dominated by a convoluted band composed by peaks at 856 and 872 cm^{-1}. So, considering this doublet, the ND9.33 phase approaches a B-type-silicate [9]. However, these two bands are too overlapped concerning those observed for typical B-type oxyorthosilicates as Lu_2SiO_5 (LSO) or Yb_2SiO_5 (YSO) [9]. Thus, the $Nd_{9.33}(SiO_4)_6O_2$ phase can hardly be considered a pure B-type oxyorthosilicate.

The performed electrical measurements (Fig. 2) agree with what would be expected according to the revised literature, since the typical response of ionic conductors with a p-type electronic behaviour [2,3,6,11] was observed. As such, the AC conductivity increased with frequency and temperature for all samples, ranging between 10^{-4} S/cm at room temperature to 10^{3} S/cm at 1000 °C (Fig. 2a). On the other hand, the high densification provided by the LFZ method [8–10] and the different polarization mechanisms [2] promote a decrease of the dielectric constant with frequency, along with an increase with temperature for all samples (Fig. 2b), varying from 1 (at RT) to 10^{9} at 1000 °C. These results confirm that local variations in the Nd phases, due to pulling rates, lead to changes in the interstitial oxygen amounts, affecting the electrical response near the room temperature, vanishing for higher temperatures [11].

Conclusions

Biphasic fibres presenting monoclinic $P2_1/c$ Nd_2SiO_5 and hexagonal $P6_3/m$ $Nd_{9.33}(SiO_4)_6O_2$ phases have been obtained for the first time by the Laser Floating Zone method (LFZ) in air changing the pulling rate from 10 to 400 mm/h. This parameter only significantly affects texture while the phase distribution barely varied. Raman spectra were recorded for the first time enabling to assign the Nd_2SiO_5 phase to an A-type oxyorthosilicate structure, while the non-stoichiometric $Nd_{9.33}(SiO_4)_6O_2$ phase approached a B-type vibrational behaviour. Electrical measurements put in evidence a p-type electronic conductivity for all samples. These results put in evidence that the materials developed are adequate for microwave dielectric devices due to the insulating character of the stoichiometric phase.

CRediT authorship contribution statement

F. Rey-García: Conceptualization, Investigation, Writing - original draft. **N.M. Ferreira:** Investigation, Writing - review & editing. **A.J.S. Fernandes:** Investigation, Writing - review & editing. **F.M. Costa:** Supervision, Funding acquisition, Writing - review & editing.

Declaration of Competing Interest

The authors declare that they have no known competing financial interests or personal relationships that could have appeared to influence the work reported in this paper.

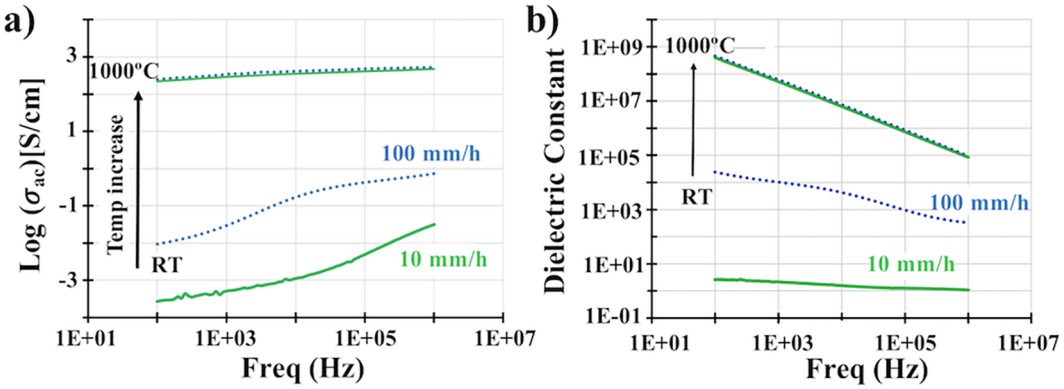

Fig. 2. Example of frequency and temperature dependence measure from 30 (RT) – 1000 ˚C in 100 ˚C steps for AC conductivity (a) and dielectric constant (b), for samples grow at 10 (green line) and 100 (dashed blue line) mm/h.

Acknowledgements

We acknowledge support from FEDER funds (COMPETE 2020 Programme) and the FCT - Portuguese Science and Technology Foundation (UIDB/50025/2020 and UIDP/50025/2020).

Appendix A. Supplementary data

Supplementary data to this article can be found online at https://doi.org/10.1016/j.rinp.2020.103180.

References

[1] Saal JE. Thermodynamic modelling of the reactive sintering of Nd:YAG [MSc Thesis]. Pennsylvania (PA) USA: Pennsylvania State University; 2008.
[2] Jiang C, et al. J. Alloys Compd. 2012;544:141–4.
[3] Oranska OI, et al. Chem. Phys. Tech Surf. 2017;8:376–83.
[4] An T, et al. Chem. Mater. 2013;25:1109–20.
[5] P. Ptácek Apatites and their Synthetic Analogues: Synthesis, Structure, Properties and Applications, Intechopen ISBN: 2016 10.5772/59882 978-953-51-2266-1.
[6] Imaizumi K. Theoretical study of oxygen ion conduction mechanisms in apatite-type oxide [Thesis]. Nagoya: Univeristy Nagoya (Japan); 2017.
[7] de la Fuente GF, et al. Solid State Ion. 1989;32–33:494–505.
[8] Rey-García F, et al. Opt. Mater. Express 2017;7:868–79.
[9] Rey-García F, et al. J. Eur. Ceram. Soc. 2018;38:2059–67.
[10] Rasekh S, et al. Mater. Des. 2015;75:143–8.
[11] León-Reina L, et al. J. Solid State Chem. 2008;181:2501–6.